

Universal limiting transition temperature for the high T_c superconductors

Moon-Sun Nam and Arzhang Ardavan

The Clarendon Laboratory, Department of Physics,

University of Oxford, Oxford OX1 3PU, UK

(Dated: February 17, 2022)

arXiv:2010.00572v1 [cond-mat.supr-con] 1 Oct 2020

Abstract

Since their discovery three decades ago it has emerged that the physics of high- T_c cuprate superconductors is characterised by multiple temperature scales, and a phenomenology that deviates significantly from the conventional paradigm of superconductivity [1–3]. Below the “pseudogap” temperature, T^* , a range of experiments indicate a reduction in the density of states [4]. Lower in temperature, T_c marks the onset of a bulk zero-resistance state. Intermediate between these, numerous other temperature boundaries and cross-overs have been identified, often postulated to be associated with fluctuations of some kind [1, 2]. However, for the most part there is little consensus either over their definitions or the physical mechanisms at play. One of these temperature scales is the Nernst onset temperature, T_{onset} , below which thermoelectric phenomena characteristic of superconductivity are observed. Depending on the material, the difference between T_{onset} and T_c ranges from almost nothing to over 100 K. In this paper, we identify T_{onset} from published experimental data according to a consistent definition; this reveals a remarkable consistency of behaviour across the whole high- T_c family, despite the appreciable variations in other parameters. Our analysis suggests that in the cuprates there is an inherent limit to $T_c \sim 135$ K. We compare this behaviour with other strongly-correlated superconductors and propose a unified picture of superconducting fluctuations close to the Mott state.

The Nernst effect, the transverse electric field E_y generated by crossed temperature gradient $\nabla_x T$ and magnetic field B_z ,

$$E_y = -e_N \nabla_x T = -N B_z \nabla_x T \quad (1)$$

where e_N is the Nernst signal and N is the Nernst coefficient. In the normal state, $N = N_n = -\frac{\pi^2}{3} \frac{k_B^2 T}{m} \frac{\partial \tau}{\partial \epsilon} \Big|_{\epsilon_F}$ is usually expected to be small (though its magnitude can be enhanced under some circumstances [5–9]), magnetic field independent for small fields, and linear in temperature [10].

A qualitatively larger signal is expected in a superconducting vortex liquid state, because the flow of heat-carrying vortices down a temperature gradient generates a transverse phase-slip. An appreciable Nernst coefficient $N = N_s + N_n$ is measured above T_c in many high- T_c materials [6] and some other strongly correlated superconductors [5]. The extra contribution N_s has been interpreted by some as indicating the presence of a phase fluctuating superconducting state; in this state, the superconducting phase is postulated to be suffi-

ciently coherent to support vortices (i.e., presumably, the phase correlation-length exceeds the superconducting coherence length defining the dimensions of a vortex core), but does not exhibit the long-range order required for a bulk zero-resistance state [11–13]. Others have argued that Gaussian fluctuations of the amplitude of the superconducting order parameter should also lead to an appreciable Nernst signal [14, 15], and there has been some debate over whether the Nernst effect observed above T_c arises from phase- or amplitude-fluctuations of the order parameter. In reality it seems likely that both fluctuation mechanisms are at play in different materials and different temperature regimes, but the consensus has emerged that the significant Nernst contribution N_s is characteristic of superconducting fluctuations. In contrast to N_n , N_s is expected to increase rapidly as temperature decreases, and to develop a magnetic field dependence.

Here, we have reviewed the extensive literature on the Nernst effect in high- T_c superconductors, and we have extracted T_{onset} from all high- T_c families for which data are reported. We have attempted to use a consistent definition, where T_{onset} is identified as the temperature at which there is a deviation of N from linearity in temperature. When the magnetic field dependence is also reported, we find that in most cases, this definition of T_{onset} is coincident with the temperature at which a magnetic field dependence emerges in N . We note in Table 1 which criterion we used to extract T_{onset} . Most values for T_{onset} that we extract are in a good agreement with the original identifications [16].

In Fig. 1 we plot the ratio of T_{onset}/T_c against T_c . A striking trends emerges: T_{onset}/T_c is clustered strongly along a line $T_{\text{onset}}/T_c \sim T_c^{-0.79}$. The common behaviour across this broad range of materials is striking. If T_{onset} marks the temperature below which there are significant superconducting fluctuations, a picture emerges of a class of materials in which what varies is how effectively they realise the “potential” for a phase-coherent superconducting state. Materials lying to the left of Fig. 1, and exhibiting a large T_{onset}/T_c ratio, fail to stabilise a coherent state until temperatures well below the onset of fluctuations. In contrast, materials to the right of the plot, typically the more three-dimensional structures with multiple of Cu-O layers, establish the long-range superconducting order at the temperature closer to the temperature at which fluctuations become significant.

The materials exhibiting the larger values of T_{onset}/T_c are generally the more two-dimensional, under-doped, single layered cuprates, and this limit is most naturally described in a phase-fluctuating picture [11–13, 18]. However, this description is less applicable to

the more three-dimensional and optimally- or over-doped materials, where an amplitude-fluctuating scenario could be more relevant, and is partially successful in describing the behaviour of optimally-doped materials [14, 15]. It is likely that a “hybrid” description is necessary for a quantitative account of the fluctuating state across the range of Fig. 1, but to our knowledge such a description does not yet exist.

We note that the trend-line for T_{onset}/T_c crosses 1 at about 135 K at the upper limit, the maximum ambient-pressure transition temperature found experimentally more than two decades ago in Hg-based superconductors ($\text{HgBa}_2\text{Ca}_2\text{Cu}_3\text{O}_{1+x}$ with $T_c \sim 133$ K) [26]. This supports the picture that across the families of cuprate superconductors there is some kind of intrinsic temperature scale (of the order 100 K) representing the “potential” for superconductivity, and that this potential is fully realised under certain circumstances of doping and crystal structure or dimensionality. This would also argue against the possibility that the cuprates are a good system in which to search for superconductors with T_c exceeding this intrinsic scale (an observation that is borne out by the history of the evolution of the maximum T_c in these materials).

Fig. 2 shows how T_{onset} varies with hole concentration p , for all samples plotted in Fig. 1 for which doping data are available. T_{onset} is clustered between 75 K and 125 K for most materials, a much narrower range than the corresponding range of T_c . The dashed line in Fig. 2 shows the ambient-pressure superconducting phase boundary as a function of p for the highest T_c Hg-based cuprate superconductors. The striking observation is that the values of T_{onset} for a very wide range of materials and dopings are clustered around the maximum T_c found in any ambient-pressure cuprate superconductor.

Within each family of materials, we find that T_{onset} has a weak dependence on p (see Fig. 2 inset showing this for LSCO), exhibiting a maximum at $p \sim 0.125$, whereas T_c is maximum at $p \sim 0.16$. The occurrence of the peak in T_{onset} at lower p than the peak in T_c suggests that the physical mechanisms determining T_{onset} are shared with those determining both T^* and T_c . Thus, the enhancement of T^* below optimum p acts to enhance T_{onset} , while at lower p , T_c is suppressed significantly, and, since T_{onset} is ultimately related to the superconductivity, T_{onset} is also eventually suppressed as p decreases. The fact that T_{onset} seems to be connected to both T^* and T_c for the entire family of materials suggests that the pseudogap is involved in the superconductivity. (We note in passing that the peak in T_{onset} is approximately coincident with the doping at which charge order is most stable [28–31]).

In summary, we have identified a consistent behaviour in the Nernst effect across a wide range of high- T_c superconductors. First, we find that T_{onset}/T_c follows a consistent trend across the family and that T_{onset} is limited at around 135K, close to the highest ambient-pressure T_c observed in the cuprate superconductors. Second, the p dependence of T_{onset} across each of the high- T_c families indicates that the superconducting fluctuation temperature scale peaks at $p \sim 0.125$, lower than the doping optimising T_c , indicating an interplay between the two temperature scales T_c and T^* .

Broadly, T_{onset}/T_c is larger for materials with lower doping (i.e., closer to the Mott state) and in which doping-dependent charge order occurs. The phase coherence of a superconducting state is associated with uncertainty in particle number [3], while in the Mott and charge-ordered states (which are stabilised by Coulomb interactions), number-uncertainty incurs an energy penalty. Thus proximity to a Mott or charge-ordered state might be expected to enhance phase fluctuations in the superconducting state.

Of course, the cuprates are not the only materials to exhibit superconductivity in the proximity of a Mott or charge-ordered state. The κ -phase quasi-two-dimensional BEDT-TTF organic molecular metals [32] offer a complementary family of strongly-correlated superconductors, in which the Coulomb energy scale, U , is set largely by the dimerised packing of the BEDT-TTF molecules. The hybridisation between the dimer orbitals sets the band width energy scale, t (see Fig. 3), and this quantity is tuneable by hydrostatic or chemical pressure, yielding a phase diagram in which a Mott state can be tuned into a strongly-correlated superconductor as a function of t/U (see Fig. 3). With further (hydrostatic or chemical) pressure, the correlation effects can be reduced further, and, eventually, the superconductivity is completely suppressed.

Throughout the κ -phase series the stoichiometry is preserved, so this family of materials gives us the opportunity to explore the phase diagram along an axis orthogonal to that relevant for the cuprates (see Fig. 3). In particular, Nernst measurements on these materials reveal a fluctuating superconducting state neighbouring the Mott state along the t/U axis [33, 34] (compounds κ -(BEDT-TTF) $_2$ Cu[N(CN) $_2$]]Cl $_{1-x}$ Br $_x$ and κ -(BEDT-TTF) $_2$ Cu[N(CN) $_2$]Br); further increasing t/U seems to suppress the fluctuating state, yielding a system in which there is no sign of fluctuations above T_c (κ -(BEDT-TTF)-Cu(NCS) $_2$).

The organics exhibit an equivalent trend in T_{onset}/T_c to what we have identified above in the cuprates in Fig. 1. There is much less Nernst data published on organics, but what is

available is plotted in Fig. 3. However, whereas in the cuprates T_{onset} is rather uniform, in the κ -(BEDT-TTF) materials T_{onset} varies greatly. It is therefore all the more remarkable that the plot of T_{onset}/T_c nevertheless seems to follow a trend analogous that exhibited in the cuprates, $T_{\text{onset}}/T_c \sim T_c^{-0.79}$ with maximum possible $T_c \sim 12$ K

This observation motivates the hypothesis that the unifying t/U vs doping phase diagram is as shown in Fig. 4. Here, we have normalised the vertical (temperature axis) to the Mott ordering temperature at zero doping (cuprates) and at minimum bandwidth (organics). Experiments show that there is a fluctuating superconducting state neighbouring the Mott state along both the t/U axis and the doping axis. The argument that proximity to the Mott state enhances superconducting phase fluctuations should apply throughout, so we suggest that the fluctuating state in organics is connected to the fluctuating state in cuprates. As yet, we do not know of an experimental system in which we can probe this bridging regime. However, recent experiments on films on κ -BEDT-TTF materials have allowed both doping (by gating the sample) and the application of strain [35, 36], offering the tantalising possibility of examining the fluctuating superconducting state as a continuous function of both t/U and doping.

We also note that in the cuprates literature there is significant variation in the reported temperature scales associated with phenomena such as charge order and fluctuation Nernst effect. Both are expected to be sensitive to magnetic field, which suppresses superconductivity but stabilises charge order [37]. The wide range of fields at which the reported experiments are conducted may therefore be masking trends; there would be value in experiments probing these temperature scales conducted at uniform (low) magnetic fields.

-
- [1] Lee, Patrick A., Nagaosa, Naoto and Wen, Xiao-Gang. Doping a Mott insulator: Physics of high-temperature superconductivity. *Rev. Mod. Phys* **78**, 17-85 (2006).
 - [2] Keimer, B. *et al.* From quantum matter to high-temperature superconductivity in copper oxides. *Nature* **518**, 179 (2015).
 - [3] Tinkham, M. *Introduction to Superconductivity* (Dover Publications, 2004), 2nd edn. (2004).
 - [4] Timusk, T. and Statt, B. The pseudogap in high-temperature superconductors: an experimental survey. *Reports on Progress in Physics* **62**, 61-122 (1999).

- [5] Behnia, K. The Nernst effect and the boundaries of the Fermi liquid picture. *J. Phys.: Condens. Matter* **21**, 113101 (2009).
- [6] Behnia, K. and Aubin, H. Nernst effect in metals and superconductors: a review of concepts and experiments. *Rep. Prog. Phys.* **79**, 046502 (2016).
- [7] Cyr-Choinière, Olivier *et al.* Enhancement of the Nernst effect by stripe order in a high- T_c superconductor. *Nature* **458**, 743-745 (2009).
- [8] Chang, J. *et al.* Nernst and Seebeck Coefficients of the Cuprate Superconductor $\text{YBa}_2\text{Cu}_3\text{O}_{6.67}$: A Study of Fermi Surface Reconstruction. *Phys. Rev. Lett.* **104**, 057005 (2010).
- [9] Daou, R. *et al.* Broken rotational symmetry in the pseudogap phase of a high- T_c superconductor. *Nature* **463**, 519 (2010).
- [10] Sondheimer, E. H. The Theory of the Galvanomagnetic and Thermomagnetic Effects in Metals *Proceedings of the Royal Society of London. Series A, Mathematical and Physical Sciences*, **193**, 484-512 (1948).
- [11] Emery, V. J. and Kivelson, S. A. Importance of phase fluctuations in superconductors with small superfluid density. *Nature* **374**, 434-437 (1995).
- [12] Wang, Yayu, Li, Lu & Ong, N. P. Nernst effect in high- T_c superconductors. *Phys. Rev. B* **73**, 024510 (2006).
- [13] Wang, Y. *et al.* Onset of the vortexlike Nernst signal above T_c in $\text{La}_{2-x}\text{Sr}_x\text{CuO}_4$ and $\text{Bi}_2\text{Sr}_{2-y}\text{La}_y\text{CuO}_6$. *Phys. Rev. B* **64**, 224519 (2001).
- [14] Ullah, Salman and Dorsey, Alan T., Critical fluctuations in high-temperature superconductors and the Ettingshausen effect. *Phys. Rev. Lett.* **65**, 2066-2069 (1990).
- [15] Ussishkin, Iddo and Sondhi, S. L. and Huse, David A. Gaussian Superconducting Fluctuations, Thermal Transport, and the Nernst Effect. *Phys. Rev. Lett.* **89**, 287001 (2002).
- [16] The advantage to identifying T_{onset} by the magnetic-field-dependent criterion is that it is absolutely empirical; it does not depend on any assumptions or models except the Gaussian fluctuations with $1/B$ dependency. Unfortunately most studies do not report a magnetic field dependence.
- [17] Capan, C. *et al.* Entropy of Vortex Cores Near the Superconductor-Insulator Transition in an Underdoped Cuprate. *Phys. Rev. Lett.* **88**, 056601 (2002).
- [18] Xu, X.A. *et al.* Vortex-like excitations and the onset of superconducting phase fluctuation in underdoped $\text{La}_{2-x}\text{Sr}_x\text{CuO}_4$. *Nature* **406**, 486-488 (2007).

- [19] Li, Lu *et al.* Unusual Nernst Effect Suggesting Time-Reversal Violation in the Striped Cuprate Superconductor $\text{La}_2\text{Ba}_x\text{CuO}_4$. *Phys. Rev. Lett.* **107**, 277001 (2011).
- [20] Okada, Y. *et al.* Enhancement of superconducting fluctuation under the coexistence of a competing pseudogap state in $\text{Bi}_2\text{Sr}_{2-x}\text{R}_x\text{CuO}_y$. *Phys. Rev. B* **81**, 214520 (2010).
- [21] Wang, Y. *et al.* Field-Enhanced Diamagnetism in the Pseudogap State of the Cuprate $\text{Bi}_2\text{Sr}_2\text{CaCu}_2\text{O}_{8+\delta}$ Superconductor in an Intense Magnetic Field. *Phys. Rev. Lett.* **95**, 247002 (2005).
- [22] F. Rullier-Albenque, R. Tourbot, H. Alloul, P. Lejay, D. Colson, and A. Forget, *Phys. Rev. Lett.* **96**, 067002 (2006).
- [23] Xu, Z. A. *et al.* Nernst effect and superconducting fluctuations in Zn-doped $\text{YBa}_2\text{Cu}_3\text{O}_{7-\delta}$. *Phys. Rev. B* **72**, 144527 (2005).
- [24] Li, Pengcheng *et al.* Correlation between incoherent phase fluctuations and disorder in $\text{Y}_{1-x}\text{Pr}_x\text{Ba}_2\text{Cu}_3\text{O}_{7-\delta}$ epitaxial films from Nernst effect measurements. *Phys. Rev. B* **75**, 184509 (2007).
- [25] Matusiak, M. *et al.* Influence of the pseudogap on the Nernst coefficient of $\text{Y}_{0.9}\text{Ca}_{0.1}\text{Ba}_2\text{Cu}_3\text{O}_y$. *EPL* **86**, 17005 (2009).
- [26] Schilling, A., Cantoni, M., Guo, J. D. and Ott, H. R. Superconductivity above 130 K in the Hg-Ba-Ca-Cu-O system. *Nature* **363**, 56–58 (1993).
- [27] Hübner, S. *et al.* Two gaps make a high-temperature superconductor? *Rep. Prog. Phys* **71**, 062501 (2008).
- [28] Kivelson, S. A. *et al.* How to detect fluctuating stripes in the high-temperature superconductors. *Rev. Mod. Phys.* **75**, 1201–1241 (2003).
- [29] Fradkin, Eduardo, Kivelson, Steven A. and Tranquada, John M. Colloquium: Theory of intertwined orders in high temperature superconductors. *Rev. Mod. Phys.* **87**, 475–482 (2015).
- [30] Wang, Yuxuan *et al.* Pair density waves in superconducting vortex halos. *Phys. Rev. B* **97**, 174510 (2018).
- [31] Dai, Zhehao *et al.* Pair-density waves, charge-density waves, and vortices in high- T_c cuprates. *Phys. Rev. B* **97**, 174511 (2018).
- [32] Ishiguro, T, Yamaji K. And Saito G. *Organic Superconductors* (Springer), 2nd edn. (2006).
- [33] Nam, Moon-Sun *et al.* Fluctuating superconductivity in organic molecular metals close to the Mott transition. *Nature* **449**, 584 (2007).

- [34] Nam, Moon-Sun *et al.* Superconducting fluctuations in organic molecular metals enhanced by Mott criticality *Scientific Reports* **3**, 3390 (2013).
- [35] H. M. Yamamoto *et al.* A strained organic field-effect transistor with a gate-tunable superconducting channel. *Nat. Commun.* 4:2379 doi: 10.1038/ncomms3379 (2013).
- [36] Y. Kawasugi *et al.* Two-dimensional ground-state mapping of a Mott-Hubbard system in a flexible field-effect device. *Sci. Adv.* **5**, eaav7282 (2019).
- [37] Wu, Tao *et al.* Magnetic-field-induced charge-stripe order in the high-temperature superconductor $\text{YBa}_2\text{Cu}_3\text{O}_y$. *Nature* **477**, 191 (2011).

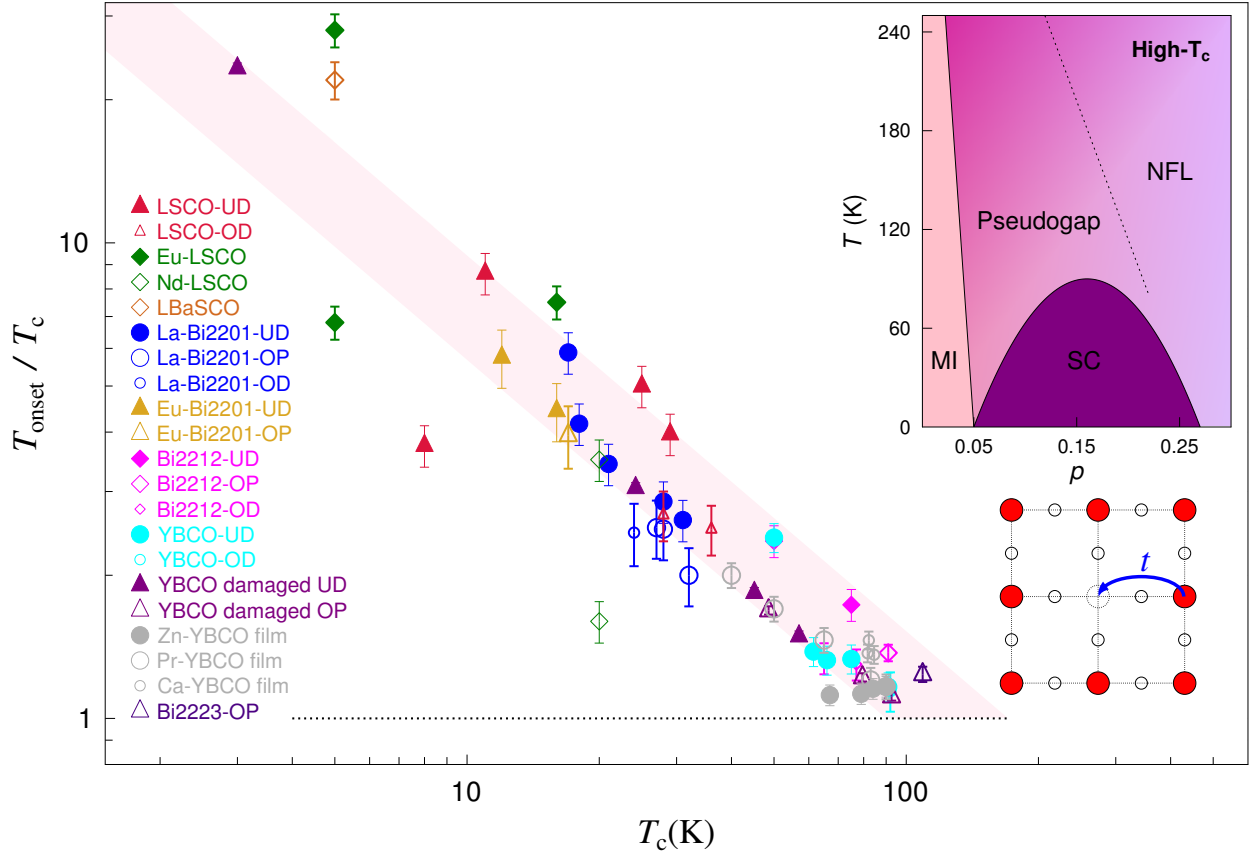


FIG. 1. Ratio of T_{onset}/T_c against T_c in high- T_c superconductors. The data are listed and referenced in Table 1 with references from which we extracted T_{onset} . “UD” indicates under-doped, “OP” optimally-doped and “OD” over-doped. Inset: the phase diagram of the cuprates as a function of hole doping and temperature.

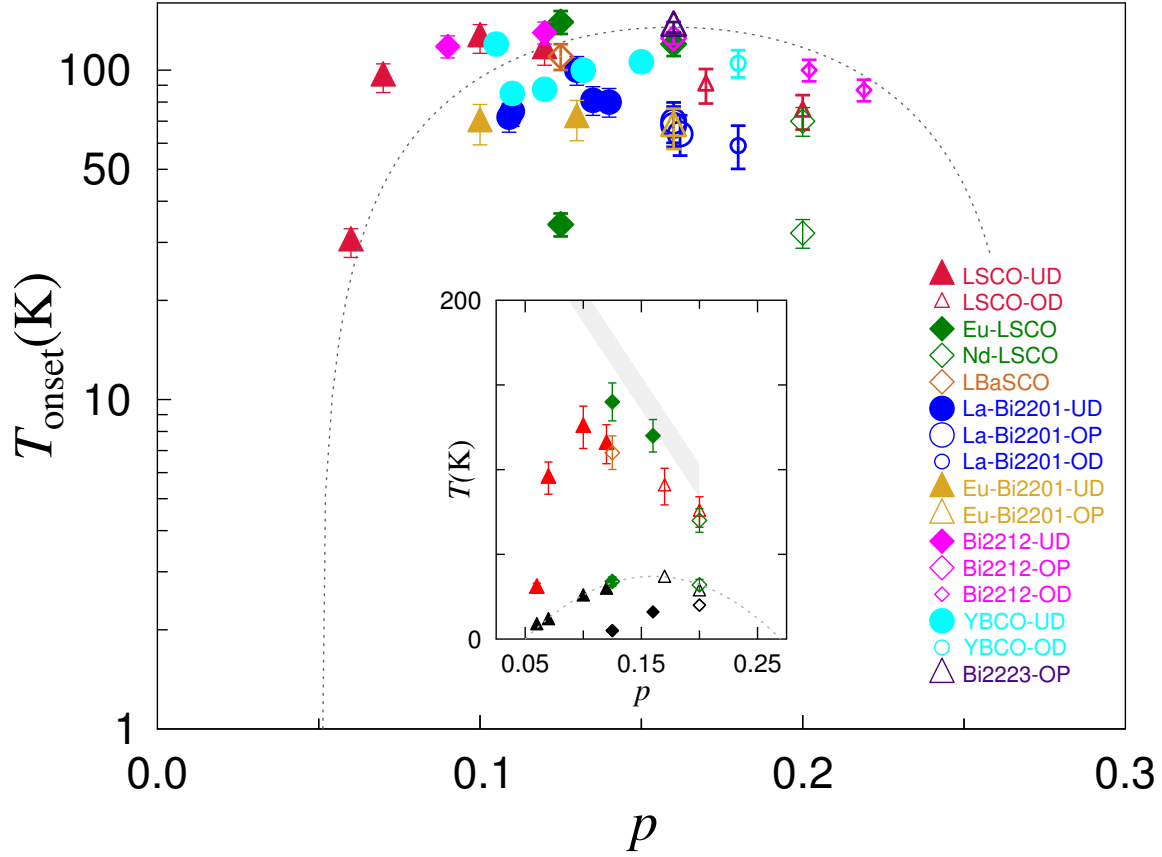


FIG. 2. T_{onset} as a function of hole concentration p . Inset: The temperatures T_c (black symbols) and T_{onset} (coloured symbols) are plotted as a function of p for a particular family, LSCO. The dotted line indicates the long-range ordered superconducting phase boundary, the grey shaded line indicates the pseudogap temperature T^* [27].

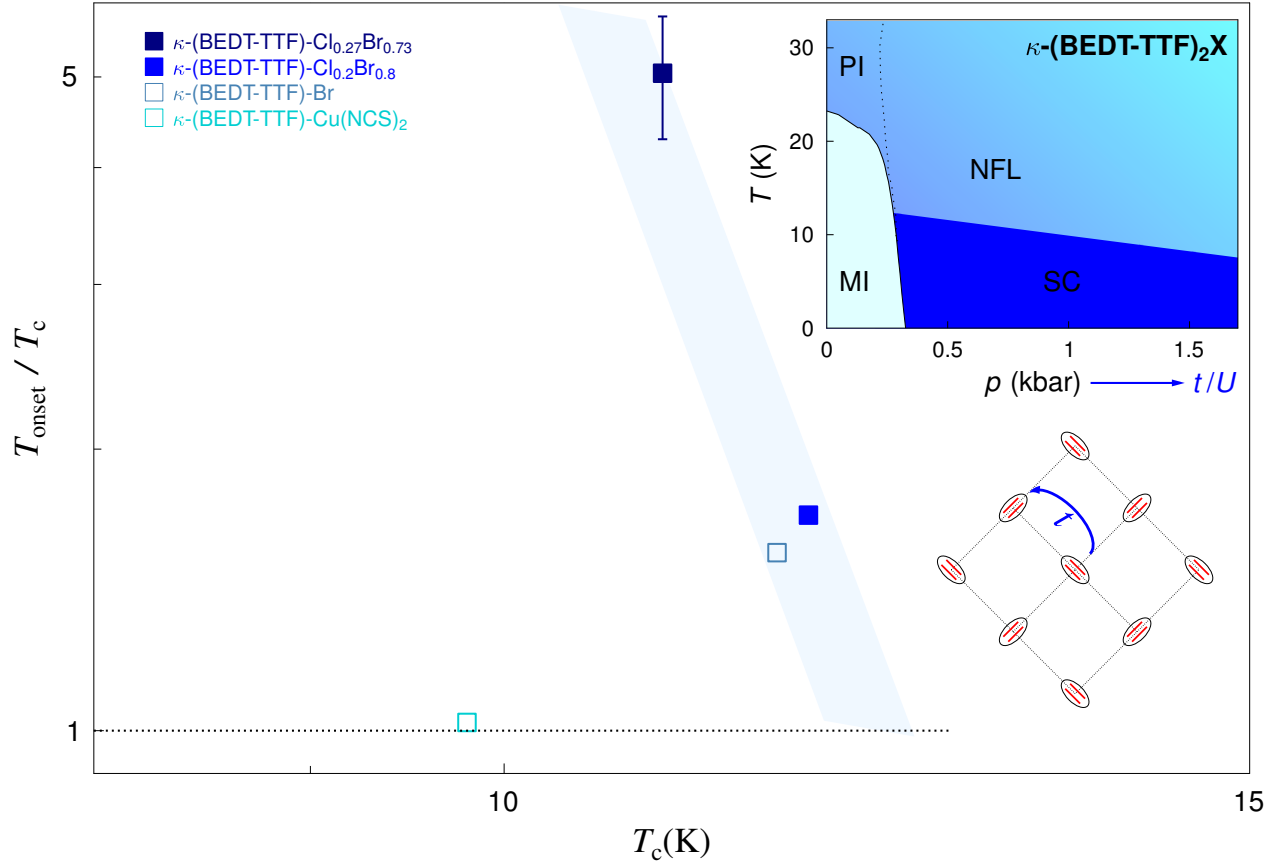


FIG. 3. Ratio of T_{onset}/T_c against T_c in κ -(BEDT-TTF) organic superconductors. The data are listed and referenced in Table 2 with references from which we extracted T_{onset} .

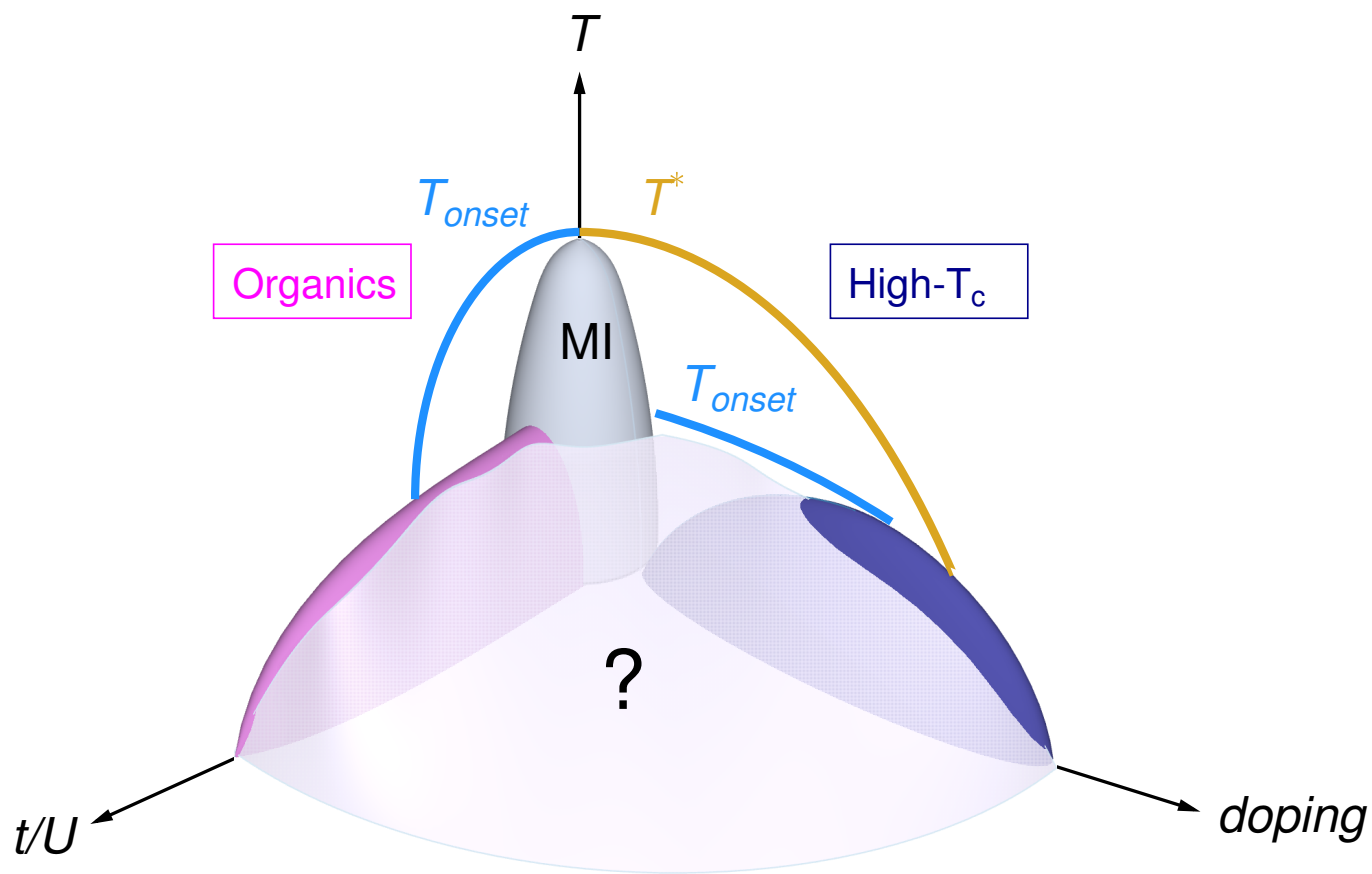


FIG. 4. Proposed unified t/U vs doping phase diagram.

	x	p	T_c (K)	T_{onset} (K)	T- linear	B-dep.	ref.
La _{2-x} Sr _x CuO ₄ UD (LSCO-UD)	0.03	0.03	0	none	○		[12]
	0.05	0.05	<4	40 ± 10	○		[12]
	0.06	0.06	8	30 ± 10	○		[17]
	0.07	0.07	11	95 ± 10	○		[12, 13]
	0.10	0.10	25	125 ± 10	○	○	[12, 18]
	0.12	0.12	29	115 ± 10	○		[12]
La _{2-x} Sr _x CuO ₄ OD (LSCO-OD)	0.17	0.17	36	90 ± 10	○		[12, 13]
	0.20	0.20	28	75 ± 10	○		[12, 13]
La _{1.8-x} Eu _{0.2} Sr _x CuO ₄ (Eu-LSCO)	0.125	0.125	5 ± 2	34 ± 4		○	[7]
	0.125	0.125	5 ± 2	140 ± 10	○		[7]
	0.16	0.16	16 ± 3	120 ± 10	○		[7]
La _{1.6-x} Nd _{0.4} Sr _x CuO ₄ (Nd-LSCO)	0.2	0.2	20 ± 1	32 ± 4		○	[7]
	0.2	0.2	20 ± 1	70 ± 4	○		[7]
La _{2-x} Ba _x CuO ₄ (LBaSCO)	0.125	0.125	5	110 ± 10	○		[19]
Bi ₂ Sr _{2-x} La _x CuO ₆ UD (La-Bi2201-UD)	0.74	0.109	21	72 ± 5	○		[20]
	0.73	0.11	18	75 ± 5	○		[20]
	0.6	0.13	17	100 ± 10	○		[13]
	0.55	0.135	31	81 ± 5		○	[20]
	0.5	0.14	28	80 ± 10	○		[13]
Bi ₂ Sr _{2-x} La _x CuO ₆ OP (La-Bi2201-OP)	0.4	0.16	28	70 ± 10		○	[13]
	0.4	0.16	27	68 ± 5	○		[20]
	0.38	0.162	32	64 ± 5	○		[20]
Bi ₂ Sr _{2-x} La _x CuO ₆ OD (La-Bi2201-OD)	0.2	0.18	24	59 ± 10	○		[20]
Bi ₂ Sr _{2-x} Eu _x CuO ₆ UD (Eu-Bi2201-UD)	0.40	0.13	16	71 ± 10	○		[20]
	0.42	0.10	12	69 ± 10	○		[20]
Bi ₂ Sr _{2-x} Eu _x CuO ₆ OP (Eu-Bi2201-OP)	0.28	0.16	17	67 ± 10	○		[20]
Bi ₂ Sr ₂ CaCu ₂ O _{8+δ} UD (Bi2212-UD)		0.09	50	118 ± 5		○	[12, 21]
		0.12	75	130 ± 10	○		[12, 21]
Bi ₂ Sr ₂ CaCu ₂ O _{8+δ} OP (Bi2212-OP)		0.16	91	125 ± 5		○	[12, 21]
Bi ₂ Sr ₂ CaCu ₂ O _{8+δ} OD (Bi2212-OD)		0.202	77	100 ± 5	○		[12, 21]
		0.219	65	87 ± 10	○		[12, 21]
YBa ₂ Cu ₃ O _y UD (YBCO-UD)	6.5	0.105	50	120 ± 10	○		[12]
	6.54	0.11	61.5	85 ± 5		○	[9]
	6.67	0.12	66	87.5 ± 5		○	[8, 9]
	6.75	0.132	75	100 ± 5		○	[9]
	6.86	0.15	91	106 ± 5		○	[9]
YBa ₂ Cu ₃ O _y OD (YBCO-OD)	6.99	0.18	92	105 ± 10		○	[12]
YBa ₂ Cu ₃ O _{6.6} damaged UD (YBCO-damaged UD)	6.6		57	85 ± 2		○	[22]
	6.6		45.1	83 ± 2	○		[22]
	6.6		24.2	74	○		[22]
	6.6		3	70	○		[22]
YBa ₂ Cu ₃ O _{7.0} damaged OP (YBCO-damaged OP)	7.0		92.6	103 ± 2	○		[22]
	7.0		79.5	97 ± 2	○		[22]
	7.0		48.6	82	○		[22]
YBa ₂ (Cu _{1-x} Zn _x) ₃ O _{7-δ} film (Zn-YBCO film)	0		90	105 ± 5	○		[23]
	0.005		84	97 ± 5	○		[23]
	0.01		79	89 ± 5		○	[23]
	0.02		67	75 ± 5	○		[23]
Y _{1-x} Pr _x Ba ₂ Cu ₃ O _{7-δ} film (Pr-YBCO film)	0	0.19	90	105 ± 5	○		[24]
	0.1		83	100 ± 5	○		[24]
	0.2		65	95 ± 5		○	[24]
	0.3		50	85 ± 5	○		[24]
	0.4		40	80 ± 5	○		[24]
Y _{0.9} Ca _{0.1} Ba ₂ Cu ₃ O _y film (Ca-YBCO film)		0.12	81.7	112 ± 5	○		[25]
		0.14	84.5	115 ± 5	○		[25]
		0.2	82.2	120 ± 5	○		[25]
Bi ₂ Sr ₂ Ca ₂ Cu ₃ O _{10+δ} OP (Bi2223OP)		0.16	109	135 ± 5		○	[12]

TABLE I. High- T_c superconductors

t/U		T_c (K)	T_{onset} (K)	T-linear	B-dep.	ref.
Higher	κ -(BEDT-TTF) ₂ Cu(NCS) ₂ (κ -(BEDT-TTF)-Cu(NCS) ₂)	9.8	10 ± 1	○	○	[33]
↓	κ -(BEDT-TTF) ₂ Cu[N(CN) ₂]Br (κ -(BEDT-TTF)-Br)	11.6	18 ± 2	○	○	[33, 34]
↓	κ -(BEDT-TTF) ₂ Cu[N(CN) ₂]Cl _{0.2} Br _{0.8} (κ -(BEDT-TTF)-Cl _{0.2} Br _{0.8})	11.8	20 ± 2	○	○	[34]
Lower	κ -(BEDT-TTF) ₂ Cu[N(CN) ₂]Cl _{0.27} Br _{0.73} (κ -(BEDT-TTF)-Cl _{0.27} Br _{0.73})	10.9	55 ± 5	○	○	[34]

TABLE II. κ -(BEDT-TTF) organic superconductors